Supporting information for

Identification of the key structural element of dihydropyrimidinone core driving toward more potent Hsp90 C-terminal inhibitors

S. Terracciano,[a] M. G. Chini,[a] M. C. Vaccaro,[a] M. Strocchia,[a] A. Foglia,[a] A. Vassallo,[b] C. Saturnino,[a] R. Riccio,[a] G. Bifulco*[a‡] and I. Bruno*[a‡]

[a] Department of Pharmacy, University of Salerno, via Giovanni Paolo II, 132, 84084, Fisciano, Italy. Fax: +39 089 969602; Tel: +39 089 969741; Tel: +39 089 969743 E-mail: bifulco@unisa.it; brunoin@unisa.it

[b] Department of Science, University of Basilicata, Viale dell'Ateneo Lucano n.10, 85100 Potenza, Italy.

‡ These authors contributed equally to this work.

1. General information

All commercially available starting materials were purchased from Sigma-Aldrich and were used without any purification. All solvents used for the synthesis were of HPLC grade; they were purchased from Sigma-Aldrich and Carlo Erba Reagenti. NMR spectra were recorded on either 300 or 400 MHz Bruker Avance instruments; all compounds were dissolved in 0.5 mL of 99.8% $CDCl_3$ (Sigma-Aldrich, 99.8 Atom % D). Coupling constants (*J*) are reported in Herz, and chemical shifts are expressed in parts per million (ppm) on the delta (δ) scale relative to $CHCl_3$ (7.26 ppm for ^1H and 77.2 ppm for ^{13}C) as internal reference. Multiplicities are reported as follows: s, singlet; d, doublet; t, triplet; m, multiplet; dd, doublet of doublets. Electrospray mass spectrometry (ESIMS) was performed on a LCQ DECA TermoQuest (San Josè, California, USA) mass spectrometer. Reactions were monitored on silica gel 60 F254 plates (Merck) and the spots were visualized under UV light. Analytical and semi-preparative reversed-phase HPLC was performed on Agilent Technologies 1200 Series high performance liquid chromatography using a Synergi Fusion C18 reversed-phase column (250 x 4.60mm, 4μ, 80 Å, flow rate = 1 mL/min; 250 x 10.00mm, 10μ, 80 Å, flow rate = 4 mL/min respectively, Phenomenex®). The binary solvent system (A/B) was as follows: 0.1% TFA in water (A) and 0.1% TFA in CH_3CN (B). The absorbance was detected at 280 nm. The purity of all tested compound (>96%) was determined by HPLC analysis. All microwave irradiation experiments were carried out in a dedicated CEM-Discover® Focused Microwave Synthesis apparatus, operating with continuous irradiation power from 0 to 300 W utilizing the standard absorbance level of 300 W maximum power. The reactions were carried out in 10 mL sealed microwave glass vials. The DiscoverTM system also offers controllable ramp time, hold time (reaction time) and uniform stirring. The temperature was monitored using the CEM-Discover built-in-vertically focused IR temperature sensor. After the irradiation period, the reaction vessel was cooled rapidly (60-120 s) to ambient temperature by air jet cooling.

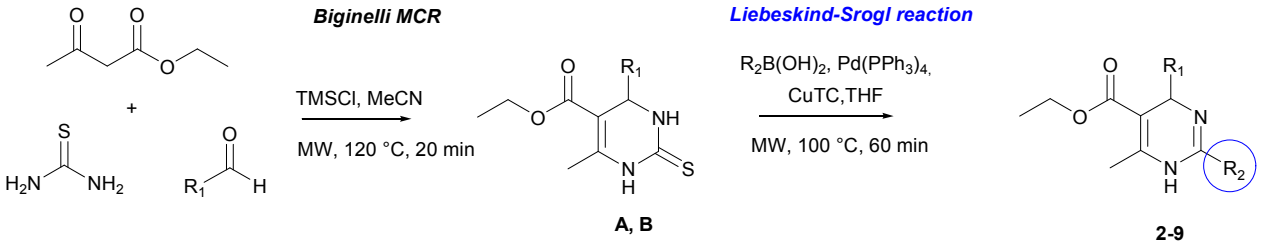

Entry	R_1	R_2	Yield[a] (%)
2	3-ethoxyphenyl	phenyl	85
3	3-ethoxyphenyl	styryl	80
4	3-ethoxyphenyl	4-(trifluoromethyl)styryl	85
5	3-ethoxyphenyl	4-fluorostyryl	75
6	3-ethoxyphenyl	4-chlorostyryl	75
7	3-ethoxyphenyl	4-methylstyryl	80
8	3-ethoxyphenyl	4-methoxystyryl	60
9	2-bromo-5-hydroxyphenyl	4-fluorostyryl	65

[a] yields of pure product after Hplc chromatography

Fig. S1 Synthesis of compound **2-9**.

2.1 Synthesis of dihydropyrimidinethione (A) through microwave-assisted Biginelli reaction[1-4]

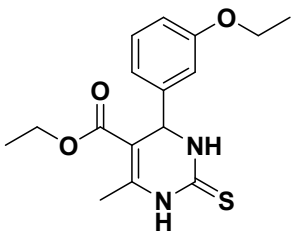

A mixture of 3-ethoxybenzaldehyde (150 mg, 1.0 mmol), thiourea (115 mg, 1.5 mmol), ethyl acetoacetate (130 mg, 1.0 mmol) in acetonitrile (1.5 mL) was placed in a 10 mL microwave glass vial equipped with a small magnetic stirring bar. TMSCl (110 mg, 1.0 mmol) was added and the mixture was then stirred under microwave irradiation at 120°C for 20 min. After irradiation, the reaction mixture was cooled to ambient temperature by air jet cooling, cold water was added and the vial was poured into crushed ice and then left at 4°C overnight. The resulting precipitate was filtered and washed with a cold mixture of ethanol/water (1:1) (3x3 mL), to give the desired product as a yellow solid in 89% yields. RP-HPLC t_R = 30.5 min, gradient condition: from 5% B to 100 % B in 50 min, flow rate of 4 mL/min, λ= 280 nm. ^{1}H NMR (300 MHz, $CDCl_3$): δ = 1.18 (t, *J* = 7.1

Hz, 3H), 1.45 (t, J = 6.9 Hz, 3H), 2.39 (s, 3H), 4.02-4.18 (m, 4H), 5.63 (s, 1H), 6.81-6.95 (m, 3H); 7.26 (t, J = 8.0 Hz, 1H). ESI-MS, calcd for $C_{16}H_{20}N_2O_3S$ 320.1; found m/z = 321.0 $[M + H]^+$.

2.2 Synthesis of dihydropyrimidinethione (B) through microwave-assisted Biginelli reaction[1-4]

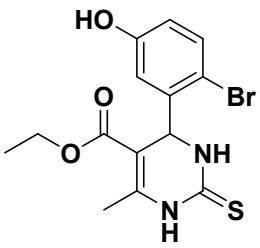

A mixture of 2-bromo-5-hydroxybenzaldehyde (200 mg, 1.0 mmol), thiourea (115 mg, 1.5 mmol), ethyl acetoacetate (130 mg, 1.0 mmol) in acetonitrile (1.5 mL) was placed in a 10 mL microwave glass vial equipped with a small magnetic stirring bar. TMSCl (110 mg, 1.0 mmol) was added and the mixture was then stirred under microwave irradiation at 120°C for 20 min. After irradiation, the reaction mixture was cooled to ambient temperature by air jet cooling, cold water was added and the vial was poured into crushed ice and then left at 4°C overnight. The resulting precipitate was filtered and washed with a cold mixture of ethanol/water (1:1) (3x3 mL), to give the desired product as a yellow solid in 89% yields. RP-HPLC t_R = 26.5 min, gradient condition: from 5% B to 100 % B in 50 min, flow rate of 4 mL/min, λ= 280 nm. ^{1}H NMR (300 MHz, $CDCl_3$): δ = 1.14 (t, J = 7.1 Hz, 3H); 2.47 (s, 3H); 4.12 (m, 2H); 5.65 (s, 1H); 6.95 (br s, 1H); 7.25 (br s, 2H). ESI-MS, calcd for $C_{14}H_{15}BrN_2O_3S$ 372.2; found m/z = 373.2 $[M + H]^+$.

3. General procedure (*a*) for microwave-assisted Liebeskind-Srogl cross coupling reaction[5-7]

A dry microwave process vial was charged with dihydropyrimidinethione **A** or **B** (1.0 equiv), the appropriate boronic acid (1.5 equiv), CuTC (3.0 equiv), and $Pd(PPh_3)_4$ (10 mol%). The reaction vessel was degassed and backfilled with nitrogen three times, and through the septum degassed dry THF (2.0 mL) was added. The mixture was subsequently heated in a microwave reactor at 100 °C for 60 min. After cooling, the mixture was transferred to a round-bottom flask and dried under reduced pressure. A solution of aqueous ammonia (25%) was added and the mixture was extracted three times with $CHCl_3$. The combined organic layers were dried with anhydrous Na_2SO_4 and

concentrated under vacuum. The crude residue was purified by HPLC to give the pure products in good yields (60-85%) and high purity (>96%).

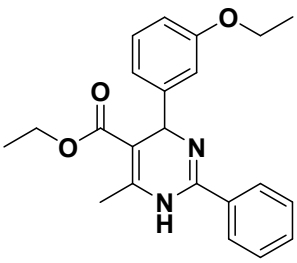

Compound **2** was obtained from **A** by following the general procedure ***a***. A portion of the crude product was then purified as follows: RP-HPLC t_R = 21.6 min, gradient condition: from 5% B to 100 % B in 50 min, flow rate of 4 mL/min, λ = 280 nm. 30.6 mg (85% yield, after HPLC purification step) as a pale yellow gelatinous solid. ^{1}H NMR (400 MHz, $CDCl_3$): δ = 1.17 (t, *J* = 7.1 Hz, 3H); 1.35 (t, *J* = 7.1 Hz, 3H); 2.50 (s, 3H); 3.93-4.01 (m, 2H); 4.07-4.16 (m, 2H); 5.66 (s, 1H); 6.80-6.90 (m, 3H); 7.19-7.30 (m, 3H); 7.47 (br s, 1H); 7.72 (br s, 2H). ^{13}C NMR (100 MHz, $CDCl_3$): δ = 15.2, 15.9, 18.0, 54.5, 61.7, 64.6, 105.4, 112.5, 117.4, 123.8, 127.1, 128.1, 129.8, 133.3, 141.4, 155.5, 163.2. ESI-MS, calcd for $C_{22}H_{24}N_2O_3$ 364.2; found m/z = 365.1 $[M + H]^+$.

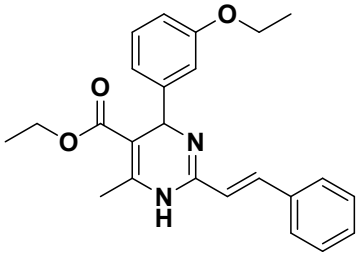

Compound **3** was obtained from **A** by following the general procedure ***a***. A portion of the crude product was then purified as follows: RP-HPLC t_R = 46.6 min, gradient condition: from 5% B to 100 % B in 80 min, flow rate of 4 mL/min, λ = 280 nm. 16 mg (80% yield, after HPLC purification step) as a pale yellow gelatinous solid. ^{1}H NMR (400 MHz, $CDCl_3$): δ = 1.13 (t, *J* = 7.1 Hz, 3H); 1.40 (t, *J* = 6.9 Hz, 3H); 2.34 (s, 3H); 4.01 (m, 4H); 5.33 (s, 1H); 6.80 (d, *J* = 6.8 Hz, 2H); 6.97 (d, *J* = 16.1 Hz, 1H); 7.21 (d, *J* = 7.9 Hz, 1H); 7.48 (s, 3H). 7.62 (m, 3H), 7.87 (d, *J* = 16.3 Hz, 1H).^{13}C NMR (100 MHz, $CDCl_3$): δ = 14.8, 15.7, 18.3, 52.7, 59.2, 62.2, 103.7, 112.0, 117.6, 118.6, 127.5, 131.3, 132.0, 141.0, 145.9, 153.1, 158.6, 162.8. ESI-MS, calcd for $C_{24}H_{26}N_2O_3$ 390.4; found m/z = 391.4 $[M + H]^+$.

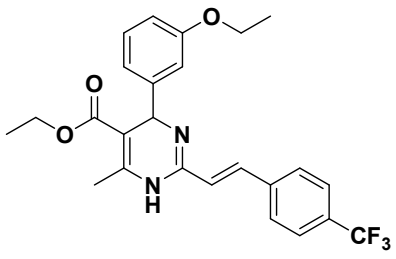

Compound **4** was obtained from **A** by following the general procedure ***a***. A portion of the crude product was then purified as follows: RP-HPLC t_R = 38.9 min, gradient condition: from 5% B to

100 % B in 70 min, flow rate of 4 mL/min, λ = 280 nm. 13 mg (85% yield, after HPLC purification step) as a pale yellow gelatinous solid. ^{1}H NMR (400 MHz, $CDCl_3$): δ = 1.12 (t, *J* = 7.1 Hz, 3H); 1.42 (t, *J* = 7.1 Hz, 3H); 2.42 (s, 3H); 4.05 (m, 4H); 5.46 (s, 1H); 6.87-6.81 (m, 3H); 6.99 (d, *J* = 16.3 Hz, 1H); 7.26 (s, 1H); 7.50 (m, 5H); 7.84 (d, *J* = 16.2 Hz, 1H). ^{13}C NMR (100 MHz, $CDCl_3$): δ = 14.8, 15.7, 18.3, 52.7, 59.2, 62.2, 103.7, 112.0, 117.6, 118.6, 127.5, 131.3, 132.0, 141.0, 145.9, 153.1, 158.6, 162.8. ESI-MS, calcd for $C_{25}H_{25}F_3N_2O_3$ 458.4; found m/z = 459.4 $[M + H]^+$

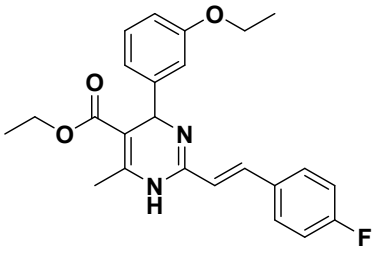

Compound **5** was obtained from **A** by following the general procedure ***a***. A portion of the crude product was then purified as follows: RP-HPLC t_R = 38.7 min, gradient condition: from 5% B to 100% B in 50 min, flow rate of 4 mL/min, λ= 280 nm. 14.8 mg (75% yield, after HPLC purification step) as a pale yellow gelatinous solid. ^{1}H NMR (300 MHz, $CDCl_3$): δ = 1.10 (t, *J* = 7.1 Hz, 3H); 1.36 (t, *J* = 7.1 Hz, 3H); 2.35 (s, 3H); 3.91-4.09 (m, 4H); 5.30 (s, 1H); 6.74-6.84 (m, 3H); 6.96 (br s, 2H); 7.20 (t, *J* = 8.0 Hz, 1H); 7.39-7.49 (m, 3H); 7.60 (br s, 1H). ESI-MS, calcd for $C_{24}H_{25}FN_2O_3$ 408.2; found m/z = 409.1 $[M + H]^+$.

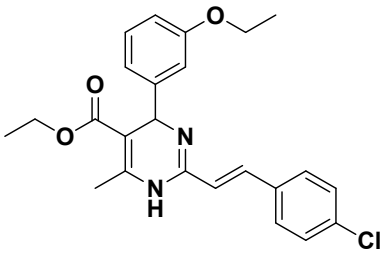

Compound **6** was obtained from **A** by following the general procedure ***a***. A portion of the crude product was then purified as follows: RP-HPLC t_R = 37.4 min, gradient condition: from 5% B to 100 % B in 70 min, flow rate of 4 mL/min, λ = 280 nm. 10 mg (75% yield, after HPLC purification step) as a pale yellow gelatinous solid. ^{1}H NMR (400 MHz, $CDCl_3$): δ = 1.15 (t, *J* = 6.9 Hz, 3H); 1.41 (t, *J* = 6.6 Hz, 3H); 2.41 (s, 3H); 4.05 (m, 4H); 5.39 (s, 1H); 6.82 (s, 1H); 7.52 (m, 4H); 7.64 (m, 5H). ^{13}C NMR (100 MHz, $CDCl_3$): δ = 14.8, 15.7, 18.3, 52.7, 59.2, 62.2, 103.7, 112.0, 117.6, 118.6, 127.5, 131.3, 132.0, 141.0, 145.9, 153.1, 158.6, 162.8. ESI-MS, calcd for $C_{24}H_{25}ClN_2O_3$ 424.9; found m/z = 425.5 $[M + H]^+$

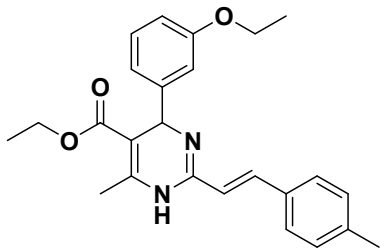

Compound **7** was obtained from **A** by following the general procedure ***a***. A portion of the crude product was then purified as follows: RP-HPLC t_R = 29.8 min, gradient condition: from 5% B to 100 % B in 50 min, flow rate of 4 mL/min, λ = 280 nm. 10 mg (70% yield, after HPLC purification step) as a pale yellow gelatinous solid. ^{1}H NMR (400 MHz, $CDCl_3$): δ = 1.09 (t, *J* = 7.1 Hz, 3H); 1.19 (t, *J* = 6.9 Hz, 3H); 2.32 (s, 3H); 2.38 (s, 3H); 4.02 (m, 4H); 5.33 (s, 1H); 6.81 (brs, 2H); 7.10 (d, *J* = 7.4 Hz, 2H); 7.25 (m, 3H); 7.42 (d, *J* = 7.7 Hz, 3H). 7.83 (d, *J* = 16.0 Hz, 1H). ^{13}C NMR (100 MHz, $CDCl_3$): δ = 14.8, 15.7, 18.6, 22.4, 54.9, 61.4, 64.1, 104.0, 111.0, 112.2, 113.2, 120.5, 128.1, 130.8, 132.1, 141.6, 145.9, 148.3, 153.8, 158.9, 162.4. ESI-MS, calcd for $C_{25}H_{28}N_2O_3$ 404.5; found m/z = 405.4 $[M + H]^+$.

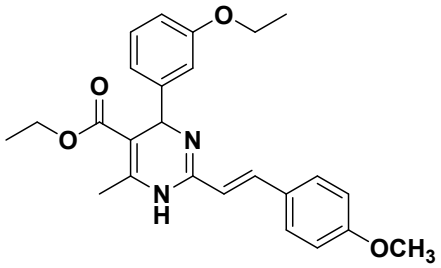

Compound **8** was obtained from **A** by following the general procedure ***a***. A portion of the crude product was then purified as follows: RP-HPLC t_R = 48.8 min, gradient condition: from 5% B to 30% B in 5 min, increased to 100 % B in 60 min, flow rate of 4 mL/min, λ = 280 nm. 8 mg (60% yield, after HPLC purification step) as a pale yellow gelatinous solid. ^{1}H NMR (400 MHz, $CDCl_3$): δ = 1.09 (t, *J* = 7.1 Hz, 3H); 1.19 (t, *J* = 6.9 Hz, 3H); 2.32 (s, 3H); 3.50 (s, 3H); 4.02 (m, 4H); 5.33 (s, 1H); 6.81 (s, 2H); 7.10 (d, *J* = 7.4 Hz, 2H); 7.25 (m, 3H); 7.42 (d, *J* = 7.7 Hz, 3H). 7.83 (d, *J* = 16.0 Hz, 1H). ^{13}C NMR (100 MHz, $CDCl_3$): δ = 14.8, 15.6, 18.2, 55.5, 61.2, 64.4, 104.1, 114.2, 117.6, 118.6, 127.5, 131.3, 132.0, 141.0, 145.9, 153.1, 158.6, 162.8. ESI-MS, calcd for $C_{25}H_{28}N_2O_4$ 420.5; found m/z = 421.5 $[M + H]^+$.

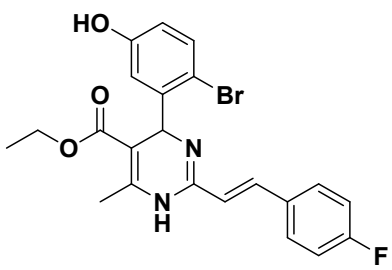

Compound **9** was obtained from **B** by following the general procedure ***a***. A portion of the crude product was then purified as follows: RP-HPLC t_R = 26.6 min, gradient condition: from 5% B to 100 % B in 50 min, flow rate of 4 mL/min, λ = 280 nm. 10 mg

(65% yield, after HPLC purification step) as a pale yellow gelatinous solid. ^{1}H NMR (300 MHz, $CDCl_3$): δ = 1.19 (t, *J* = 7.1 Hz, 3H); 2.69 (s, 3H); 4.12 (m, 2H); 5.94 (s, 1H); 6.72 (m, 2H); 6.92 (s, 1H); 7.07 (t, *J* = 8.1 Hz, 1H); 7.36 (d, *J* = 8.5 Hz, 1H); 7.53 (d, *J* = 7.2 Hz, 2H); 7.85 (d, *J* = 16.4 Hz, 1H). ESI-MS, calcd for $C_{22}H_{20}BrFN_2O_3$ 459.3; found m/z = 365.1 $[M + H]^+$

4. Surface Plasmon Resonance Analyses

Recombinant human Hsp90α was purchased from Abcam (Abcam, Cambridge, UK). Proteomic grade trypsin was purchased from Sigma-Aldrich (Sigma-Aldrich Co, St Louis, MO, USA). The Hsp90 inhibitor 17-(Allylamino)-17-demethoxygeldanamycin (17-AAG) was purchased from Sigma-Aldrich and used in SPR experiments as a positive control.

SPR analyses were carried out according to our previously published procedures[2,8-11] and were performed using a Biacore 3000 optical biosensor equipped with research-grade CM5 sensor chips (GE Healthcare). Using this platform, two separate recombinant Hsp90α surfaces, a BSA surface and one unmodified reference surface were prepared for simultaneous analyses. Proteins (100 μg mL^{-1} in 10 mM CH_3COONa, pH 5.0) were immobilized on individual sensor chip surfaces at a flow rate of 5 μL min^{-1} using standard amine-coupling protocols to obtain densities of 8–12 kRU.

Compounds **2-9**, as well as 17-AAG, were dissolved in 100% DMSO to obtain 4 mM solutions, and diluted 1:200 (v/v) in PBS (10 mM NaH_2PO_4, 150 mM NaCl, pH 7.4) to a final DMSO concentration of 0.5%. Compounds concentration series were prepared as twofold dilutions into running buffer: for each sample, the complete binding study was performed using a six-point concentration series, typically spanning 0.025–1 μM, and triplicate aliquots of each compound concentration were dispensed into disposable vials. Binding experiments were performed at 25°C, using a flow rate of 50 μL min^{-1}, with 60 s monitoring of association and 300 s monitoring of dissociation (Table S1).

Simple interactions were suitably fitted to a single-site bimolecular interaction model (A+B = AB), yielding a single K_D. Sensorgram elaborations were performed using the BIAevaluation software provided by GE Healthcare.

Table S1. Thermodynamic constants measured by SPR for the interaction between tested compounds and immobilized Hsp90α.

Compound	K_D (μM)
2	No Binding
3	0.0127±0.0032
4	0.0021±0.0009
5	0.0078±0.0011
6	0.397±0.003
7	0.0181±0.0044
8	0.0065±0.0027
9	0.0475±0.0091
1a[a]	0.076±0.007
17-AAG[a]	0.388±0.089

[a] data previously reported[2]

5. Cell culture

A375, human melanoma cells and Panc-1, human pancreatic carcinoma (American Type Culture Collection, Manassa, VA) were used. Cells were cultured in Dulbecco's modified Eagle medium (DMEM) supplemented with 10% (v/v) FBS, 2mM l−glutamine and antibiotics (100 U/mL penicillin, 100 µg/mL streptomycin) purchased from Invitrogen (Carslbad, CA, USA), at 37°C in humidified atmosphere with 5% CO_2. To ensure logarithmic growth, cells were subcultured every 2 days. As control cells, human peripheral blood mononuclear cells (PBMC) were isolated from buffy coats of healthy donors (kindly provided by the Blood Center of the Hospital of Battipaglia, Salerno, Italy) by using standard Ficoll−Hypaque gradients. Freshly isolated PBMC contained 92.8 ± 3.1% live cells. Proliferation of PBMC was induced by phytohemagglutinin (PHA) (10 µg mL^{-1}).

5.1 Cell proliferation and viability assay

A375 and Panc-1cells were seeded in triplicate in 96 well−plates ($1x10^4$ /well) and incubated for the 24 h or 48 h in the absence or presence of different concentrations of compound **3-9** (concentration between 0.5 µM to 100 µM). Stock solutions of compounds (100 mM in DMSO) were stored a 4°C in the dark and diluted just before addition to the sterile culture medium. In all the experiments, final concentration of DMSO was 0.15% (v/v).

The number of viable cells was determined by using a [3-4,5-dimethyldiazol-2-yl]-2,5-diphenyl tetrazolium bromide (MTT, Sigma-Aldrich) conversion assay, according to the method described by Mosmann.[11]

Briefly, following the compound-incubation, 25 µL of MTT solution (5mg/mL in PBS) was added to each well and were incubated for additional 3 h at 37°C. Thereafter, cells were lysed and suspended with 100 µL of buffer containing 50% (v/v) N,N-dimethylformamide, 20% SDS (pH

4.5). The absorbance was measured with a microplate reader (Titertek multiskan MCC7340, LabSystems, Vienna, VA, USA) equipped with a 620 nm filter. IC_{50} values were calculated from cell viability dose−response curves and defined as the concentration resulting in 50% inhibition of cell survival, compared to control cells treated with DMSO. 17-AAG had an IC_{50} = 2 μM in A375 cell lines,[2] while 17-AAG used from 1 to 10 μM (24 h), inhibited the Panc-1 cell viability by 10 to 30%.

PBMC were treated with **3**-**5** used at the concentrations corresponding to the IC_{50} values of A375 and Panc-1 cells (2 μM or 5 μM, respectively) to evaluate their effects on non-cancer cells viability. The cell population growth inhibition was tested by cytometric counting (trypan blu exclusion).

6. Western Blot

The A375 and Panc-1 cells were incubated for 24 h with DMSO or compound **5** used at the concentrations corresponding to the IC_{50} values (2 or 5 μM, respectively). Treated cells were harvested and lysed in ice-cold RIPA buffer (50 mM Hepes, 10 mM EDTA, 150 mM NaCl, 1% NP-40, 0.5% sodium deoxycholate, 0.1% SDS, pH 7.4), supplemented with protease inhibitors cocktail (Sigma-Aldrich). The protein concentration was determined according to the Bio-Rad Protein assay (Biorad Laboratories, CA, USA) and 30 μg were separated by SDS-PAGE under denatured reducing conditions and were then transferred to nitrocellulose membranes. The western blot analysis was carried out as previously described [2]. The antibodies used were: Anti-Hsp 27; Anti-Hsp 70; anti-Hsp 90α/ß, anti-Raf, anti-pAkt, anti-actin (Santa Cruz Biotechnology, Inc., Delaware, CA, USA).

7. Cell cycle analysis

Cell DNA content was measured by propidium iodide (PI) incorporation into permeabilized cells, as described by Nicoletti et al. 1991[12]. Briefly, the cells were harvested after treatment with compound **3**-**5**, washed with cold PBS and incubated with a PI solution (0.1% sodium citrate, 0.1% Triton X-100 and 25 μg/ml of prodium iodide, Sigma-Aldrich, 10 μg/ml Rnase A) for 30 min at 4 °C. Data from 10.000 events for each sample were collected by a FACScalibur flow cytometry (Becton Dickinson, San Josè, CA) and cellular debris was excluded from analysis by raising the forward scatter threshold. Percentage of cells in the sub G_0/G_1 phase, hypodiploid region, was quantified using the CellQuest software (Becton Dickinson). The distribution of cells in G_0/G_1, S, G_2/M phases was determined using ModFit LT cell cycle analysis software (Becton Dickinson). Results were expressed as a mean ± SD of two experiments performed in triplicate.

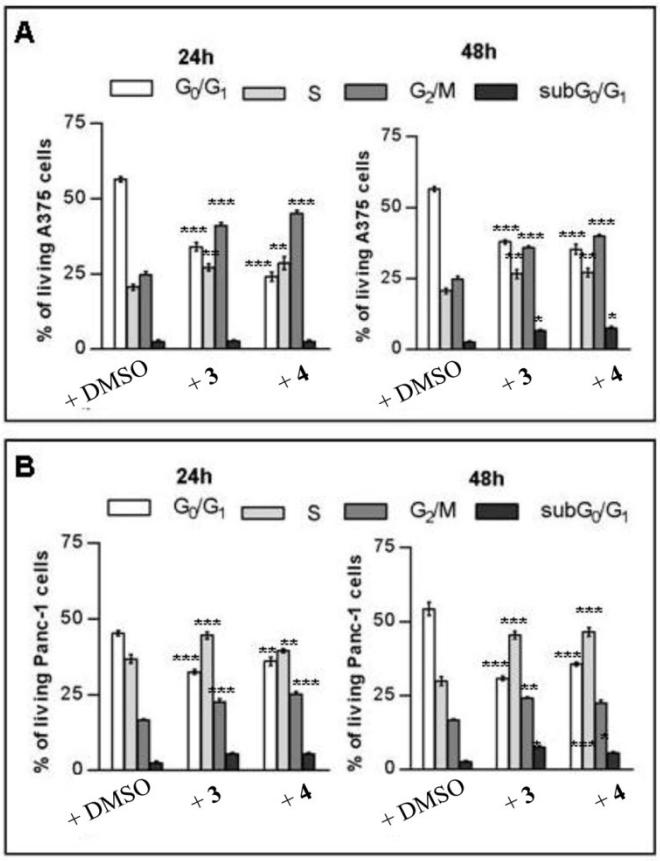

Fig. S2 Effect of compound **3** or **4** on cell cycle distribution in A375 and Panc-1 cells. Quantification of cell cycle distribution of viable A375 (A) or Panc-1(B) cells treated with DMSO, compound **3** or **4** (2 or 5μM, respectively) or 17-AAG (2 or 2.5 μM, respectively) for 24 h,

evaluated by PI staining. Results are expressed as means ± SD of three independent experiments, performed in duplicate (***P < 0.001, **P < 0.01, *P < 0.05 versus control).

8. Limited Proteolysis

Limited proteolysis experiments[2,13-15] were performed on recombinant Hsp90α at 37°C, PBS 0.1% DMSO, using trypsin or chymotrypsin as proteolytic agents; 30 mL of a 3 μM Hsp90α solution were used for each experiment. Binary complex Hsp90α/**5** or Hsp90α/Novobiocin were formed by incubating the protein with a 5:1 molar excess of **5** or Novobiocin, respectively, at 37°C for 15 min prior to proteolytic enzyme addition. Both Hsp90α, Hsp90α/**5** and Hsp90α/Novobiocin complex were digested using a 1:100 (w/w) enzyme to substrate ratio. The extent of the reactions was monitored on a time-course basis by sampling the incubation mixture after 5, 15, and 30 min of digestion. Samples were analyzed by MALDI-TOF/MS using a MALDI micro MX (Waters). Mass data were elaborated using the Masslynx software (Waters). Preferential hydrolysis sites on Hsp90α under different conditions were identified on the basis of the fragments released during enzymatic digestion.

9. Statistical analysis

All the reported data represent the mean ± standard deviation (SD) of at least two independent experiments, performed in triplicate. Where necessary, data were statistically compared by Student's t-test; the statistical significance of DNA content between cells group was examined in the two-way analysis of variance (ANOVA) with Bonferroni post-test analysis using GraphPad Prism 5 software. Differences were considered significant if $p < 0.05$.

10. Molecular docking studies

Input Files Preparation for Docking. Protein 3D model of the ATP-bound active state of Hsp82, an yeast Hsp90α homologue (PDB code: 2CG9)[16] was prepared using the Schrödinger Protein Preparation Wizard workflow.[17] Briefly, water molecules that were found 5 Å or more away from heteroatom groups were removed and cap termini were included. Additionally, all hydrogen atoms were added, and bond orders were assigned. The resulting PDB files were converted to the MAE format. Chemical structures of investigated compounds were built with Maestro's Build Panel (version 10.2)[18] and subsequently processed with LigPrep (version 3.4)[19] in order to generate all the possible tautomers and protonation states at a pH of 7.4 ± 1.0; the resulting ligands were finally minimized employing the OPLS 2005 force field.

10.1 Induced Fit Docking. Binding sites for the initial Glide docking phases (Glide Standard Precision Mode) of the Induced Fit Workflow (Induced Fit Docking, protocol 2015-2, Glide version 6.4, Prime version 3.7, Schrödinger)[20-22] were calculated on the 2CG9 structure, considering the centroid of the region site singled out by limited proteolysis for grid generation. In all cases, cubic inner boxes with dimensions of 14 Å were applied to the proteins, and outer boxes were automatically detected. Ring conformations of the investigated compounds were sampled using an energy window of 2.5 kcal/mol; conformations featuring nonplanar conformations of amide bonds were penalized. Side chains of residues close to the docking outputs (within 8.0 Å of ligand poses) were reoriented using Prime (Prime version 3.7, Schrödinger 2015), and ligands were redocked into their corresponding low energy protein structures (Glide Extra Precision Mode), considering inner boxes dimensions of 5.0 Å (outer boxes automatically detected), with resulting complexes ranked according to GlideScore. Illustrations of the 2D and 3D model were generated using Maestro software.[23]

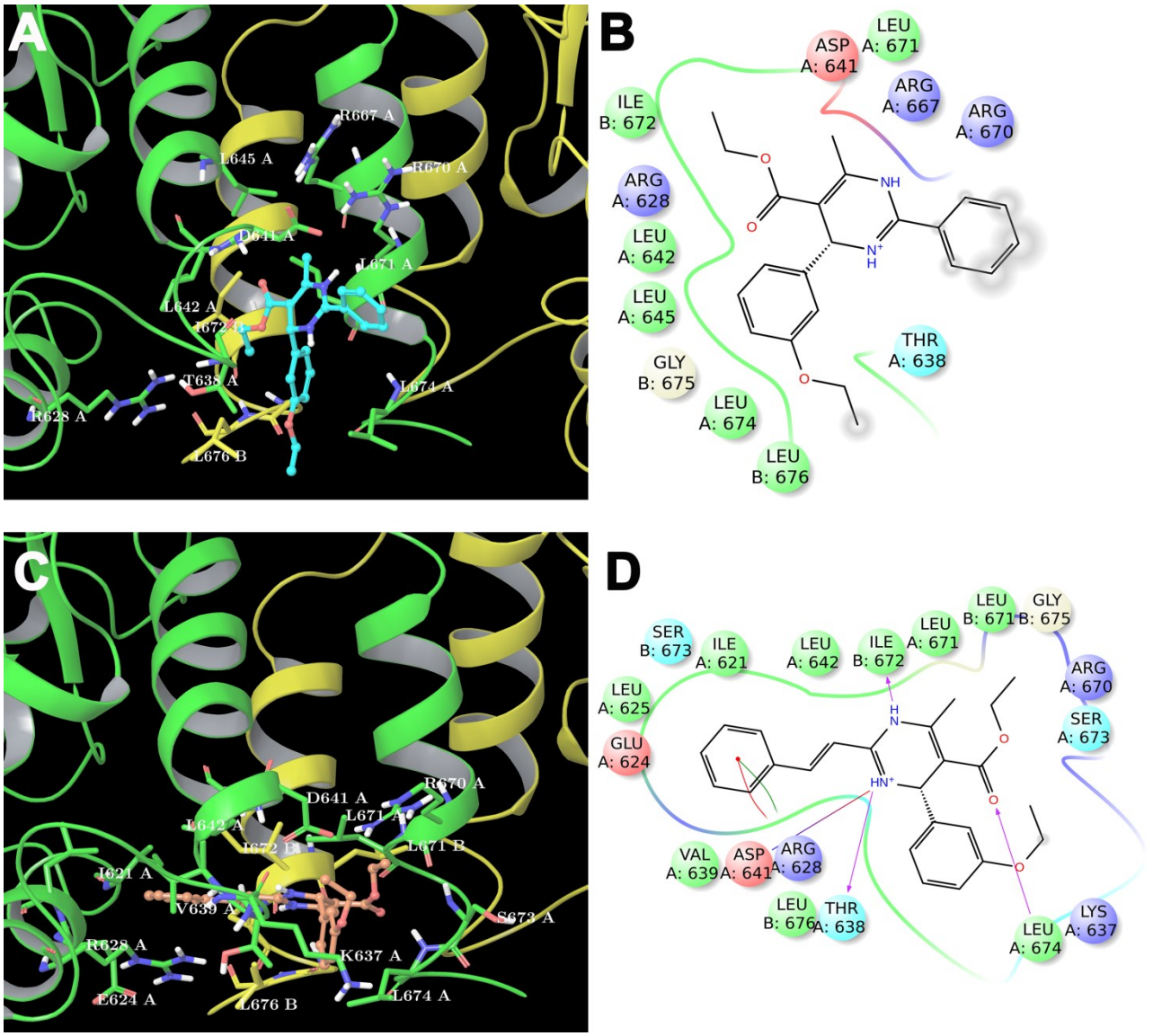

Fig. S3. Three dimensional models (panel A and C) and 2D diagram interactions (panel B and D) of **2** (cyan) and **3** (orange) with C-terminal domain of HSP82 yeast analogue of Hsp90α (PDB: 2CG9). In the panels A and C, the protein is reported as colored ribbons: chain A is depicted in green and chain B is depicted in yellow. The aminoacids interacting with each ligand are reported in green (chain A) and yellow (chain B) sticks. In the panels B and D, positive charged residues are colored in violet, negative charged residues are colored in red, polar residues are colored in light blue, hydrophobic residues are colored in green. The π-π stacking interactions are indicated as green lines, and H-bond (side chain) are reported as dotted pink arrows.

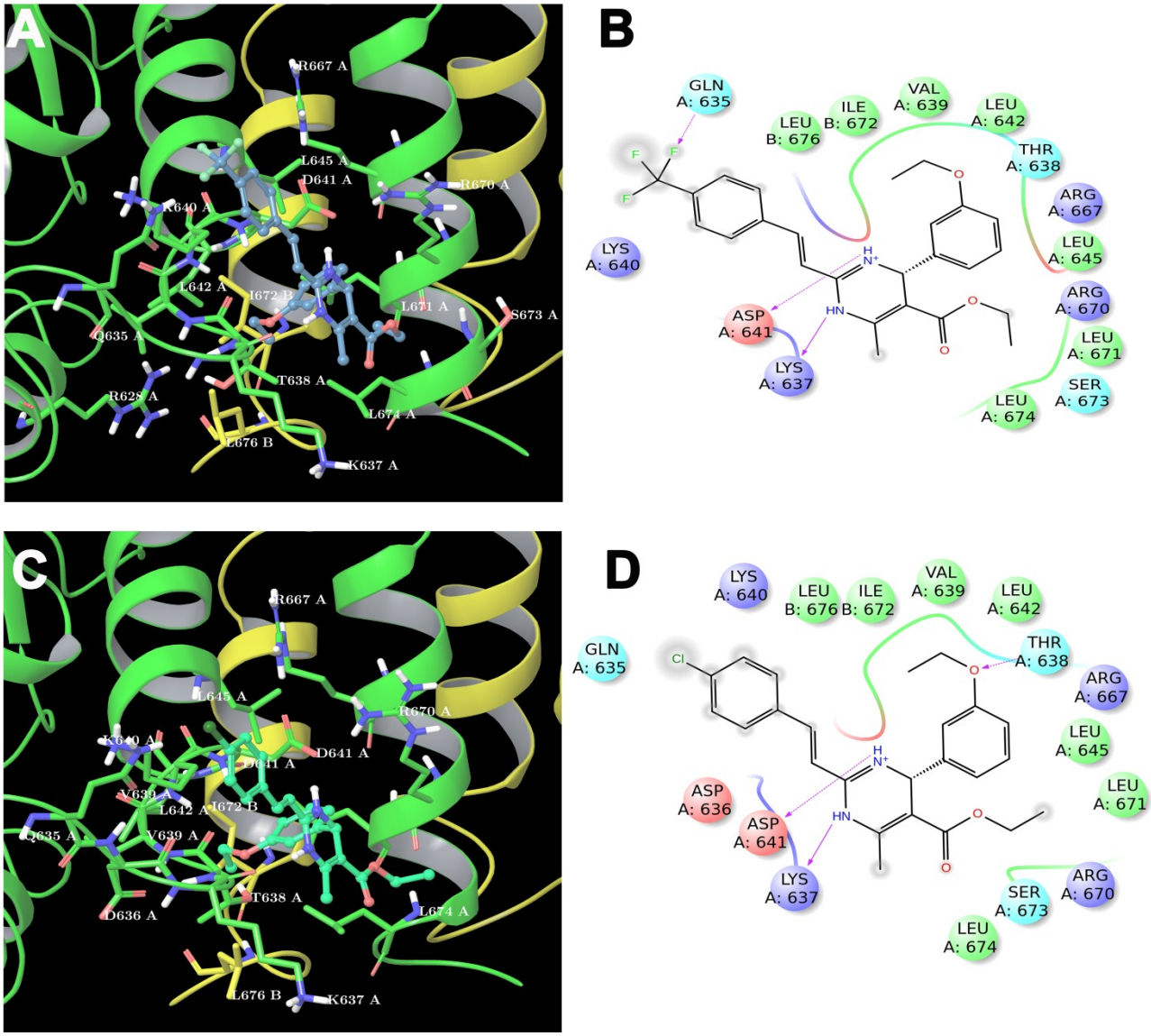

Fig. S4. Three dimensional models (panel A and C) and 2D diagram interactions (panel B and D) of **4** (blue) and **6** (light green) with C-terminal domain of HSP82 yeast analogue of Hsp90α (PDB: 2CG9). In the panels A and C, the protein is reported as colored ribbons: chain A is depicted in green and chain B is depicted in yellow. The aminoacids interacting with each ligand are reported in green (chain A) and yellow (chain B) sticks. In the panels B and D, positive charged residues are colored in violet, negative charged residues are colored in red, polar residues are colored in light blue, hydrophobic residues are colored in green. The π-π stacking interactions are indicated as green lines, and H-bond (side chain) are reported as dotted pink arrows.

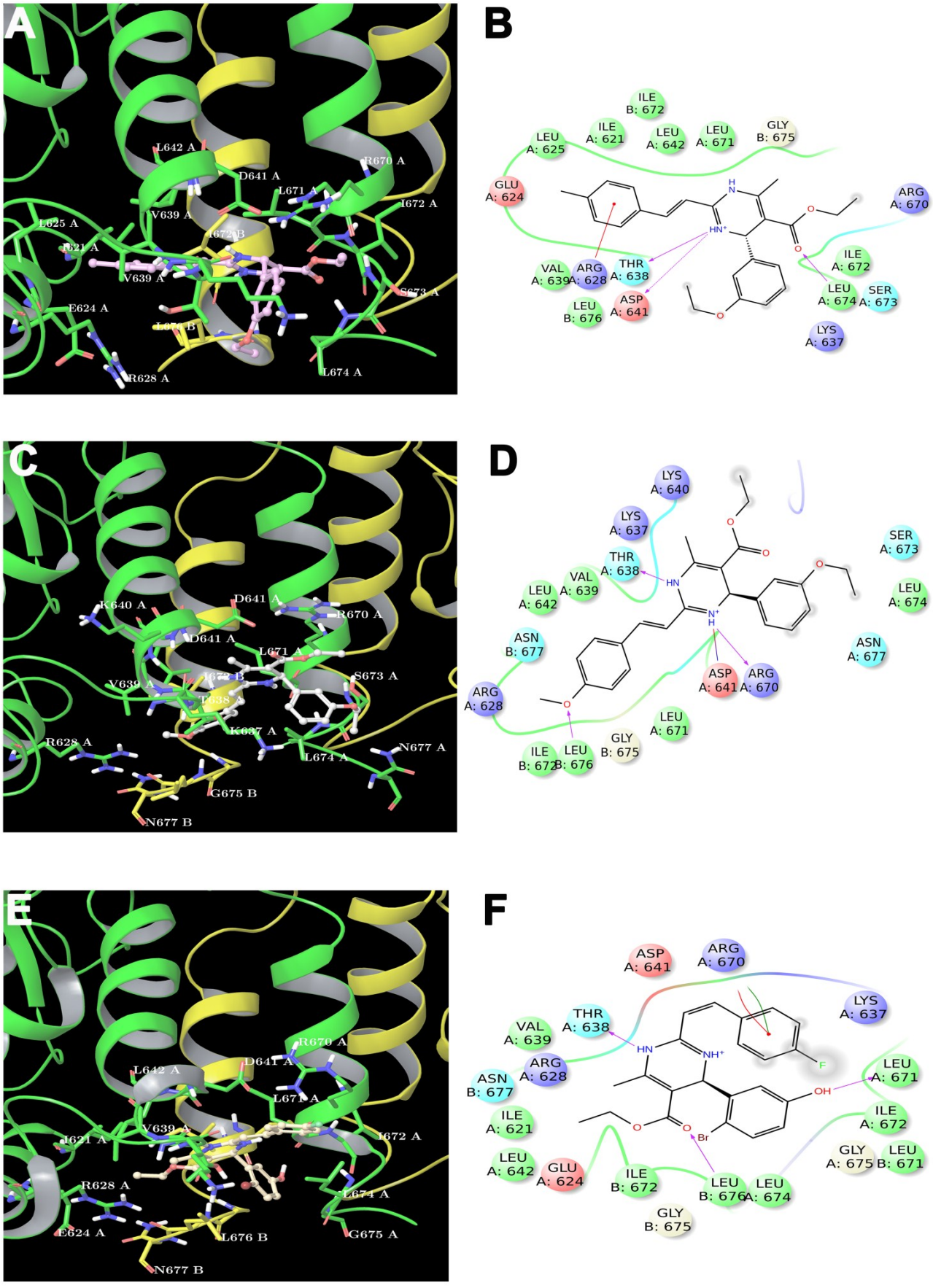

Fig. S5. Three dimensional models (panel A, C and E) and 2D diagram interactions (panel B, D and F) of **7** (pink), **8** (white), and **9** (beige) with C-terminal domain of HSP82 yeast analogue of Hsp90α (PDB: 2CG9). In the panels A, C and E, the protein is reported as colored ribbons: chain A is

depicted in green and chain B is depicted in yellow. The aminoacids interacting with each ligand are reported in green (chain A) and yellow (chain B) sticks. In the panels B, D and F, positive charged residues are colored in violet, negative charged residues are colored in red, polar residues are colored in light blue, hydrophobic residues are colored in green. The π-π stacking interactions are indicated as green lines, and H-bond (side chain) are reported as dotted pink arrows.

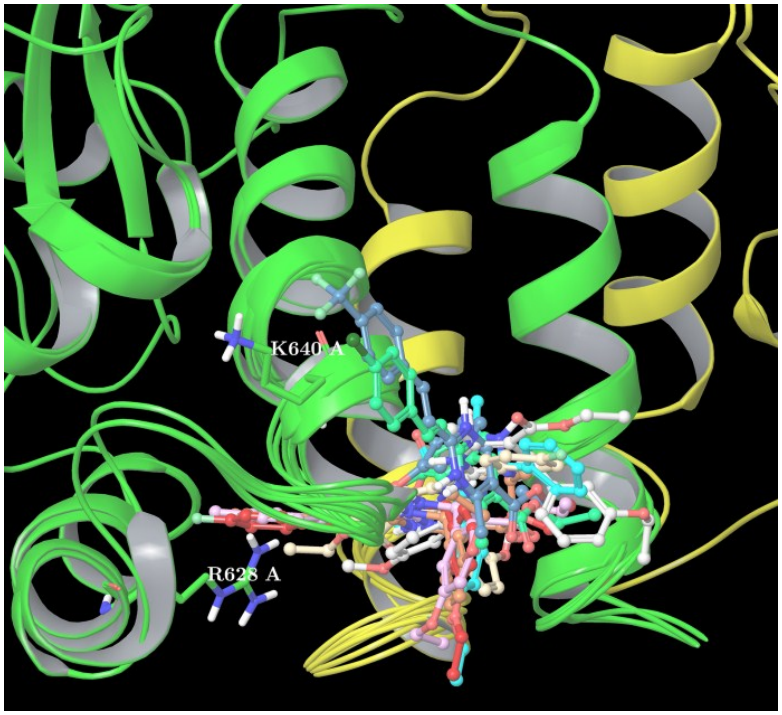

Fig. S6. Superimposition of **5** (red) with **2** (cyan), **3** (orange), **4** (blue), **6** (light green), **7** (pink), **8** (white), **9** (beige) in the C-terminal domain of HSP82 yeast analogue of Hsp90α (PDB: 2CG9).

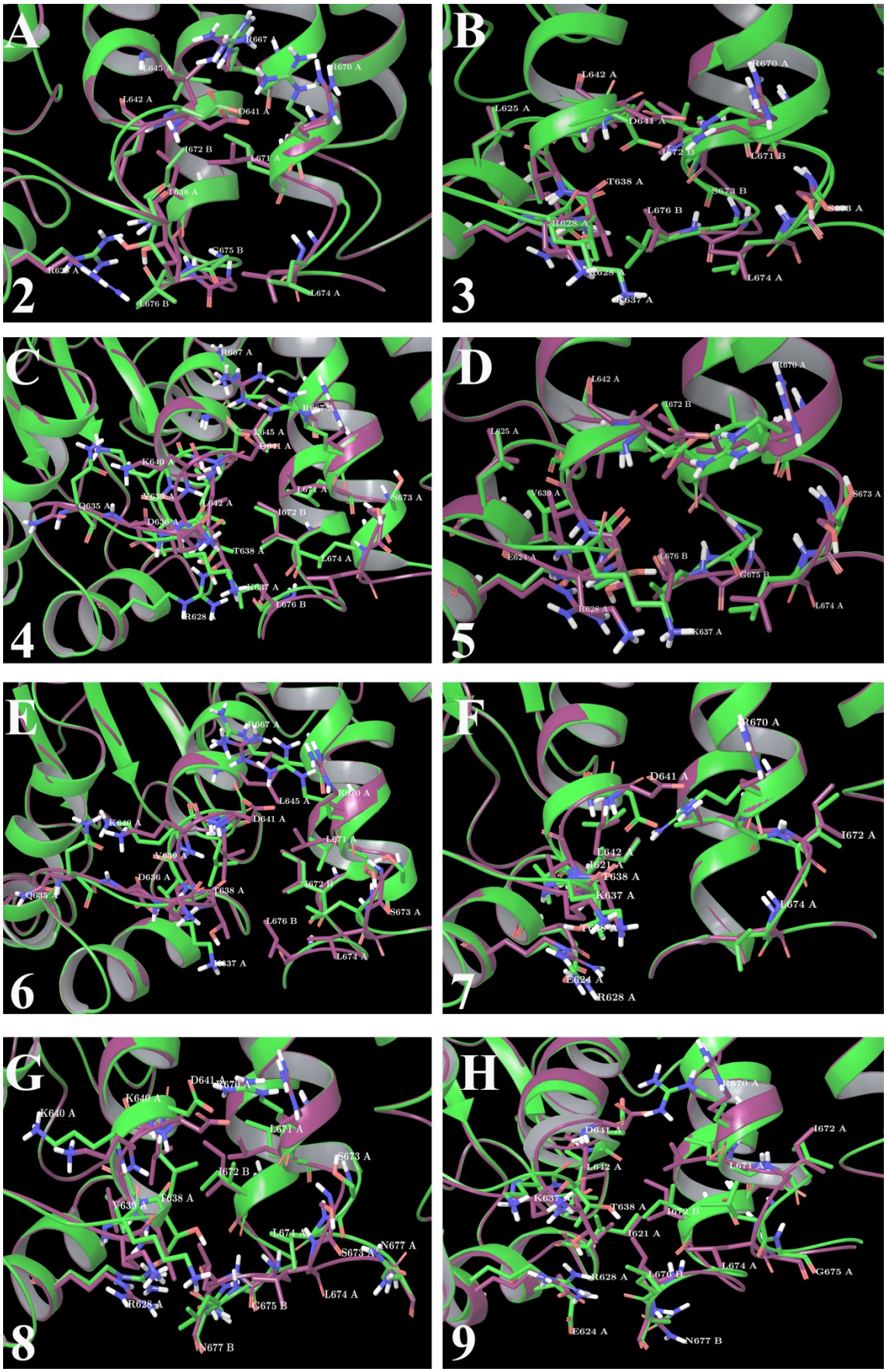

Fig. S7. Positioning of the key residues in the calculated complexes of **2-9** (ligands not shown) with C-terminal domain of HSP82 yeast analogue of Hsp90α with respect to its original X-ray structure

(PDB: 2CG9). The rigid receptor is depicted as purple ribbons and sticks, the receptor after Induced Fit Docking calculation is depicted as green ribbons and sticks.

References

1 C. O. Kappe, Eur. J. Med. Chem., 2000, 35, 1043; L. Pisani, H. Prokopcová, J. M. Kremsner and C. O. Kappe, *J. Comb. Chem.*, 2007, **9**, 415; J. P. Wan and Y. Pan, Mini-Rev. Med. Chem., 2012, **12**, 377.

2 M. Strocchia, S. Terracciano, M. G. Chini, A. Vassallo, M. C. Vaccaro, F. Dal Piaz, A. Leone, R. Riccio, I. Bruno and G. Bifulco, *Chem. Commun.,* 2015, **51**, 3850—3853.

3 G. Lauro, M. Strocchia, S. Terracciano, I. Bruno, K. Fischer, C. Pergola, O. Werz, R. Riccio and G. Bifulco, *Eur. J. Med. Chem.*, 2014, **10**, 407.

4 S. Terracciano, G. Lauro, M. Strocchia, K. Fischer, O. Werz, R. Riccio, I. Bruno, G. Bifulco, *ACS Med. Chem. Lett.*, 2015, ***6*(2)**, pp 187–191.

5 N. Arshad, J. Hashim, O. Kappe, *J. Org. Chem.* 2009, **74**, 5118-5121.

6 H. Prokopcovà, O. Kappe, *Adv. Synth. Catal* 2007, **349**, 448-452.

7 N. Arshad, J. Hashim, O. Kappe, *J. Org. Chem.* 2009**, 74**, 5118-5121.

8 A. Vassallo, M. C. Vaccaro, N. De Tommasi, F. Dal Piaz and A. Leone, *Plos One*, 2013, **8**, e74266.

9 F. Dal Piaz, A. Vassallo, L. Lepore, A. Tosco, A. Bader and N. De Tommasi, *J. Med. Chem.*, 2009, **52**, 3814.

10 S. Terracciano, M. G. Chini, F. Dal Piaz, A. Vassallo, R. Riccio, I. Bruno and G. Bifulco, *Eur. J. Med. Chem.*, 2013, **65**, 464.

11 T. Mosmann, *J. Immunol, Methods*, 1983, **65**, 55.

12 I. Nicoletti, G. Migliorati, MC. Pagliacci, F. Grignani, C. Riccardi, *J. Immunol. Methods*, 1991, **139**: 271-279.

13 S. Orrù, F. Dal Piaz, A. Casbarra, G. Biasiol, R. De Francesco, C. Steinkühler and P. Pucci, *Protein Sci*., 1999, **8**, 1445.

14 F. Dal Piaz, A. Vassallo, M. G. Chini, F. M. Cordero, F. Cardona, C. Pisano, G. Bifulco , N. De Tommasi and A. Brandi, *PLoS One*, 2012, **7(8)**, e43316.

15 F. Dal Piaz , P. Ferro, A. Vassallo, M. V., G. Forte, M. G. Chini, G. Bifulco, A. Tosco and N.De Tommasi, *Biochim. Biophys. Acta*, 2015, **1850**, 1806.

16 M. M. U. Ali, S. M. Roe, C. K. Vaughan, P. Meyer, B. Panaretou, P. W. Piper, C. Prodromou, L. H. Pearl, *Nature* 2006, **440**, 1013.

17 Schrödinger, LLC New York NY, 2015.

18 Maestro, version 10.2, Schrödinger, LLC, New York, NY, 2015.

19 LigPrep, version 3.4, Schrödinger, LLC, New York, NY, 2015.

20 W. Sherman, T. Day, M.P. Jacobson, R.A. Friesner, R. Farid, *J. Med. Chem.* 2006*,* **49**, 534.

21 W. Sherman, H.S. Beard, R. Farid, *Chem. Biol. Drug Des.*, 2006, **67**, 83.

22 Induced Fit Docking, protocol 2015-2, Glide version 6.4, Prime version 3.7, Schrödinger, LLC, New York, NY, 2015.

23 Maestro, Schrödinger, LLC, New York, NY, 2015.